

Effect of Hydrolysis Treatment on Cellulose Nanowhiskers from Oil Palm (*Elaeis guineensis*) Fronds: Morphology, Chemical, Crystallinity, and Thermal Characteristics

Chaturbhuj K. Saurabh,^a Rudi Dungani,^{b,*} A. F. Owolabi,^{a,c} N. S. Atiqah,^a A. Zaidon,^d N. A. Sri Aprilia,^e Zaidul Md. Sarker,^f and H. P. S. Abdul Khalil^a

Oil palm fronds biomass was used as a source for isolation of cellulose nanowhiskers (CNW), and its subsequent characterization was done. Non-cellulosic components such as lignin, hemicellulose, and pectin were removed from the biomass by chemimechanical alkaline hydrogen peroxide method followed by sulphuric acid hydrolysis having different time duration of hydrolysis. Apart from the progressive reduction in peaks characteristic of hemicellulose and lignin dissolution, FTIR spectroscopy analysis showed that there were no significant variations in peak positions, signifying that the hydrolysis did not affect the chemical structure of CNW. FESEM showed that there was gradual reduction in the aggregated structure of fiber due to bleaching. Nanoscale structure of CNW was revealed by TEM. XRD analysis revealed that the natural structure of cellulose I polymorph was maintained irrespective of the hydrolysis time. High thermal stability and aspect ratio of the extracted CNW demonstrated its suitability as a reinforcement material in nanocomposites.

Keywords: Oil palm frond; Cellulose nanowhiskers; Thermal analysis; FESEM; XRD; FTIR; TEM

Contact information: a: School of Industrial Technology, Universiti Sains Malaysia, Penang; b: School of Life Sciences and Technology, Gedung Labtex XI, Institut Teknologi Bandung, Indonesia; c: Federal Institute of Industrial research oshodi, Lagos Nigeria; d: Faculty of Forestry, Universiti Putra Malaysia, 43400 Serdang, Selangor, Malaysia; e: Department of Chemical Engineering, Engineering Faculty of Syiah Kuala University, Banda Aceh, Indonesia; f: Kulliyyah of Pharmacy, International Islamic University Malaysia, Kuantan Campus, 25200 Kuantan, Pahang, Malaysia;

* Corresponding author: rudi@sith.itb.ac.id

INTRODUCTION

Challenges posed by dwindling availability of non-renewable fossil resources such as petrochemical-based non-biodegradable plastics has contributed to the search for alternative polymer materials that are environmentally friendly and recyclable (Khan *et al.* 2009; Peleteiro *et al.* 2015). Polymeric composites are widely used due to their enhanced characteristics over plain polymer-based materials (Aprilia *et al.* 2015). The use of lignocellulose biomass as reinforcement for polymer composites has received attention due to their abundance and recyclability (White *et al.* 2011; Davoudpour *et al.* 2015). Recent advances in various lignocellulosic materials as fillers and reinforcement in polymers has represented a remarkable breakthrough in biopolymer-based materials. Cellulose nanowhiskers (CNW) have enticed significant attention as a reinforcement in polymer matrixes due to their exceptional blend of high physical properties and environmental benefits (Studart and Erb 2014). Conventionally, nanofibres have been extracted from cotton due to its very high cellulose content. However, being an agricultural waste, the lignocellulosic material could be a cheap source of CNW.

The term CNW is used for materials such as cellulose nanocrystals (CNC), nanocrystalline cellulose (NCC), and cellulose crystallites (CC) (Zoppe *et al.* 2014; Brioude *et al.* 2015). CNW are highly crystalline needle-shaped cellulose particles with one of its dimensions equal to or less than 100 nm (Sèbe *et al.* 2012; Chen *et al.* 2014; Xu *et al.* 2014). Even a very low amount of CNW incorporation as reinforcement material in polymer has been found to significantly improve thermal, mechanical, and barrier properties of composite materials as compared to the conventional composites (Osorio-Madrado *et al.* 2012; Chen *et al.* 2014). This can be mainly attributed to a large specific surface area, very high modulus of elasticity, and high aspect ratio of CNW.

CNW production is a two-step process. The first step is cellulose extraction, which has an equal multidimensional approach. In this step, any of the following processes can be used: chemical treatment (pulping and bleaching), chemimechanical (chemical treatment and mechanical refining action), and chemo-mechanical (chemical extraction of cellulose fibre before mechanical fragmentation of the fibre). The second step is acid hydrolysis of the extracted fibre, which was pioneered by Rånby (1951) and is the most widely used procedure (Wang and Chen *et al.* 2013; Xu *et al.* 2014; Lamaming *et al.* 2015). Acid hydrolysis process involves spontaneous dissolution of cellulose fibre into acid, based on the quicker hydrolysis kinetics (QHK) of the amorphous parts of cellulose. The acid penetrates the disordered cellulose fibre followed by breaking of its glycosidic bonds through the cleavage resulting in cellulose fibrils separation, releasing single and well-defined crystals. Natural cellulose is rich in such crystals (Khalil *et al.* 2014a). Sulphuric acid hydrolysis is characterized by the introduction of sulphate based bulky ester groups onto the hydroxyl groups of cellulose. The introduction of ester groups stabilizes the CNW in solution through the electrostatic repulsion of the charged ester groups, thereby enhancing its dispersion in water hence preventing the clustering of nanowhiskers (Eichhorn *et al.* 2010). The application of CNW as a reinforcing agent in nanocomposite depends on its morphology and properties (Eichhorn *et al.* 2010). The morphology and properties of CNW are greatly influenced by the source of fibre, acid-to-cellulose ratio in acid hydrolysis, hydrolytic temperature, hydrolysis time and the acid concentration.

Recently, researchers have reported the isolation of nanocrystalline cellulose from empty fruit bunch (EFB) using chemo-mechanical process followed by acid hydrolysis (Jonoobi *et al.* 2010; Fahma *et al.* 2011), while Haafiz *et al.* (2014) prepared CNW from micro crystalline cellulose obtained from EFB. Isolation of cellulose nanocrystals from oil palm trunk (OPT) using modified chemo-mechanical method followed by acid hydrolysis has also been reported (Lamaming *et al.* 2015). However, no study has been reported on the isolation of CNW from oil palm fronds using chemimechanical alkaline hydrogen peroxide method followed by sulphuric acid hydrolysis having different time duration of hydrolysis. The objective of this work was to investigate the effect of acid hydrolysis time on morphology, thermal, spectra, and crystallinity of the isolated CNW. The analysis included field emission scanning electron microscope (FESEM), Fourier transmission infrared spectroscopy (FTIR), crystallinity index, crystal size dimension, and thermogravimetric analysis.

EXPERIMENTAL

Materials

Freshly pruned oil palm fronds (OPF) was obtained from oil palm plantation in Perak, Malaysia. The hydrogen peroxide (30%), sodium hydroxide pellet ($\geq 97\%$), glacial

acetic acid (99.5%), sodium chlorite (NaClO_2) (80%), and sulphuric acid (98%) of Sigma-Aldrich (USA) specification were procured from local chemical vendors.

Characterization of the OPF cellulose fibre

OPF fibre was chemically analyzed by TAPPI (Technical Association of the Pulp and Paper Industry) standard methods. Prior to the chemical analysis the fibres were subjected to extractive removal with ethanol/benzene [1:2 (v/v)] using Soxhlet extraction for 6 hours. The TAPPI standard methods T 212 om-93, T 203 os-74, and T 211 om-93, were used for determining the alpha-cellulose, lignin, and ash content, respectively.

Preparation of Bleached OPF Cellulose Fibre

The supplied OPF was allowed to undergo field retting for three weeks to ease the extraction of vascular bundles of fibres. The extracted vascular bundles were cut into 4 to 5 cm lengths, washed thoroughly with distilled water at ambient temperature (30 °C), and allowed to air dried at 30 °C before packing in polyethylene bags and storage at 10 °C \pm 2.

The procedure of isolation of CNW was earlier reported by Fahma *et al.* (2011), and in the present study it was adopted and modified. Seventy grams of OPF fibres was mixed with distilled water at a fibre-to-water ratio of 1:10 and heated at 70 °C for 30 min to remove water soluble extractives from the biomass. Obtained slurry was pressed at 15 psi pressure to separate fibres from dissolved water soluble extractives. Fibre was then placed in plastic bag. A mixture of alkaline hydrogen peroxide (AHP) liquor (H_2O_2 : NaOH : 5:4 (v/w)) was prepared and added to the fibre in the plastic bag at 1:10 solid to liquor ratio.

The polyethylene bag containing reaction mixture was kept for 1 h at 70 °C. During this process lignin and hemicellulose were dissolved (Naran *et al.* 2009; Banerjee *et al.* 2011; Liu *et al.* 2015), and the resulting pulp slurry was pressed at 15 psi and refined using DD series double disc refiner (Finland Metso corporation) operated at 120 kw power at 5% consistency.

The extracted fibre was thoroughly washed with distilled water. Obtained fibres were bleached in acidified NaClO_2 solution at 70 °C for 1 h and subsequently washed with distilled water.

Isolation of CNW

CNW were isolated from the bleached OPF according to the procedure by Ellazzouzi *et al.* (2007) and Wang *et al.* (2013). Five grams of the bleached fibre was mixed with 8.75 mL/g sulphuric acid (64% w/w) with constant stirring at different time durations (15, 30, 45, and 60 min) at 45 °C. The acid hydrolysis was terminated by adding excess distilled water, and the hydrolyzed solution was filtered by fine porosity Büchner Funnel, Glass Frit (model number 60240). The filtrate was centrifuged for three cycles at 10,000 rpm for 10 min. The nanowhisker pellet was finally washed by membrane dialysis until the pH of neutrality was achieved. The prepared CNW was subjected to air drying at 30 °C for 72 h and milled for seven hours using an electrical powered Stainless steel interchangeable jar Laboratory Ball Mill equipped with hardened steel balls. The yield was expressed in weight percentage of oven dried CNW to raw OPF fibre.

Characterization

Morphology characteristics

Morphological changes in the CNW were monitored with the help of a LEO Supra 50 Vp FESEM equipped with secondary, backscattered electron and EDX detectors. The FESEM system operated in variable N₂ gas pressure. Prior to analysis samples were gold-sputtered with the aid of sputter coater model Polaron SC 515 ± 20 nm sample size thickness.

Transmission electron microscope (TEM)

A Philips CM 12 device was used to measure the structural dimension distribution of the CNW. A drop of sonicated diluted OPF-CNW was placed on copper grids coated with a carbon support film for observation. The specimens were stained with one small drop of 2% uranyl acetate to improve the viewing contrast while excess liquid stain on the copper grid surface was blotted by filter paper. A total of 20 fibres of each sample were measured and the result was reported as the mean with their standard deviation values.

Thermal Analysis

Thermal stability tests of the CNWs were carried out using 9 mg of each sample by means of Perkin-Elmer TGA 7. Thermal decomposition of the CNWs was observed between temperature ranging from room temperature to 800 °C at a heating rate of 10 °C/min under N₂ atmosphere to prevent any thermoxidative degradation of samples.

Fourier Transform Infrared (FTIR) Spectroscopy Analysis

Changes in chemical constituent of CNWs fibre were monitored with the aid of a Nicolet infrared spectrophotometer (Avatar 360 FT-IR E.S.P). About 1 mg of the sample were pulverised and mixed with 99 mg of KBr. The mixture was then introduced into a hollow chamber and pressed to make a small pellet. The spectra produced were in transmittance mode between wave numbers 4000 cm⁻¹ to 400 cm⁻¹.

X-ray diffraction (XRD) analysis

The crystallinity index (CrI) of the dried CNW powder was analyzed using XRD with Ni-filtered CuKα radiation (wavelength of 1.5406 Å) at 40 kV and 40 mA. The 2θ ranges from 5° to 60°, samples were scanned at 2° per minute. The crystallinity index CrI was calculated according to Segal *et al.* (1959), using Eq. 1,

$$CrI(\%) = \frac{(I_{002} - I_{am})}{I_{002}} \times 100 \quad (1)$$

where I_{002} and I_{am} are the peaks intensity correspond to crystalline and amorphous fractions respectively. The average crystallite size in crystalline region was calculated from the Scherrer equation (Eq. 2):

$$D_{002} = \frac{k\lambda}{B_{002} \cos \theta} \quad (2)$$

Taking k as the Scherrer constant (0.84), λ is the X-ray wavelength (1.54 nm), B in radians is the full width at half maximum (FWHM) of I_{002} diffraction peak and θ the corresponding Bragg angle.

Statistical analysis

Obtained results were evaluated using analysis of variance (ANOVA) followed by Duncan's multiple range test at 95% confidence while all the data were reported as mean with the standard deviations (\pm SD). Three samples were taken for every treatment and each sample was further analyzed in triplicates.

RESULTS AND DISCUSSION

Chemical Analysis

Comparative chemical analysis of OPF biomass with respect to other oil palm biomass is presented in Table 1. It was observed that all the oil palm biomass exhibited high cellulose content, which is an advantage for its suitability as alternative source to cotton or microcrystalline cellulose for the extraction of CNWs (Law *et al.* 2007; Abdul Khalil *et al.* 2008; Hashim *et al.* 2010). OPF vascular bundles have lower lignin and hemicellulose contents compared to the other fibrous oil palm biomass; this is an added advantage for easy extraction of CNWs. Thus in the present study, OPF was used for the extraction of nanowhiskers using bleaching and hydrolysis.

Table 1. Chemical Composition of Oil Palm Biomass

| | OPF | EFB ¹ | OPT ² |
|---------------------------|----------------------------|------------------|------------------|
| Acid insoluble lignin (%) | 17.72 \pm 3.30 % (n = 5) | 18.8 \pm 0.3 | 24.51 |
| Ash content (%) | 4.79 \pm 0.59 % (n = 5) | 1.3 \pm 0.2 | 2.2 |
| Alpha cellulose (%) | 54.66 \pm 9.71% (n = 5) | 62.9 \pm 2.0 | 41.02 |
| Hemicellulose (%) | 23.52 \pm 0.2 % (n = 5) | 28.0 | 29.50 |

(¹Law *et al.* 2007 and ²Abdul Khalil *et al.* 2008)

Electron Microscopy

Surface morphology of fibers might change during chemical and mechanical pre-treatment. The FESEM images of raw and bleached fiber are shown in Fig 1.

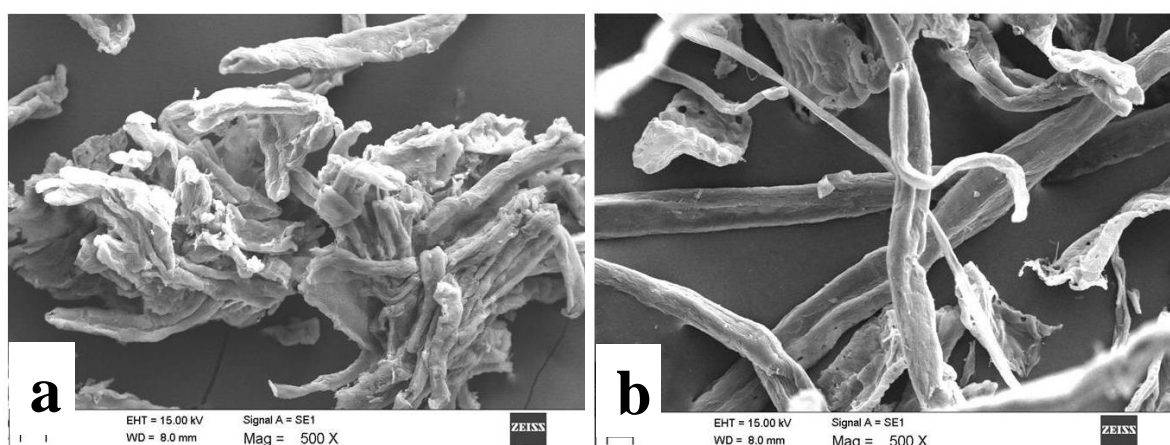


Fig. 1. FESEM images of (a) raw fiber (b) bleached fiber

The images reveal that there were morphological changes in fibers during the bleaching process. Raw bamboo fiber is mainly composed of lignin, hemicelluloses, and waxy materials (Mustafa *et al.* 2011), which typically gave rough and irregular surface to raw fiber (Fig 1a). The surface of fibers appear to be uniform and smooth in SEM image

of bleached fiber (Fig 1b) due to removal of non-cellulosic materials. This also resulted in liberation of individual fibers cemented by non-cellulosic materials.

TEM images of the nanowhiskers suggest that the acid hydrolysis resulted in removal of amorphous and non-crystalline impurities such as pectin and hemicellulose that constitute the cementing components around the raw fibre bundles. Acid hydrolysis successfully removed amorphous regions from fibre through transverse cleavage of microfibril fibres into free and individualized CNW (Battista 1950; Battista and Smith 1962). As the hydrolysis time increased, the observed number of CNW also increased. Table 2 shows the comparison between dimensions of extracted CNW by different hydrolysis times from OPF fibre with other common lignocellulose fibres. The result shows that there was gradual reduction in the yield of the CNW as the hydrolysis time increased. In the present study, the yield of CNW-45 was higher than an earlier report on OPT by Lamaming *et al.* (2015). This improvement in the yield could be attributed to the modification in extraction procedure of CNW. Furthermore, diameter of CWN had a gradual decrease as the hydrolysis time increases. This might be due to the progressive removal of the amorphous portion of cellulose fibre with increase in hydrolysis time.

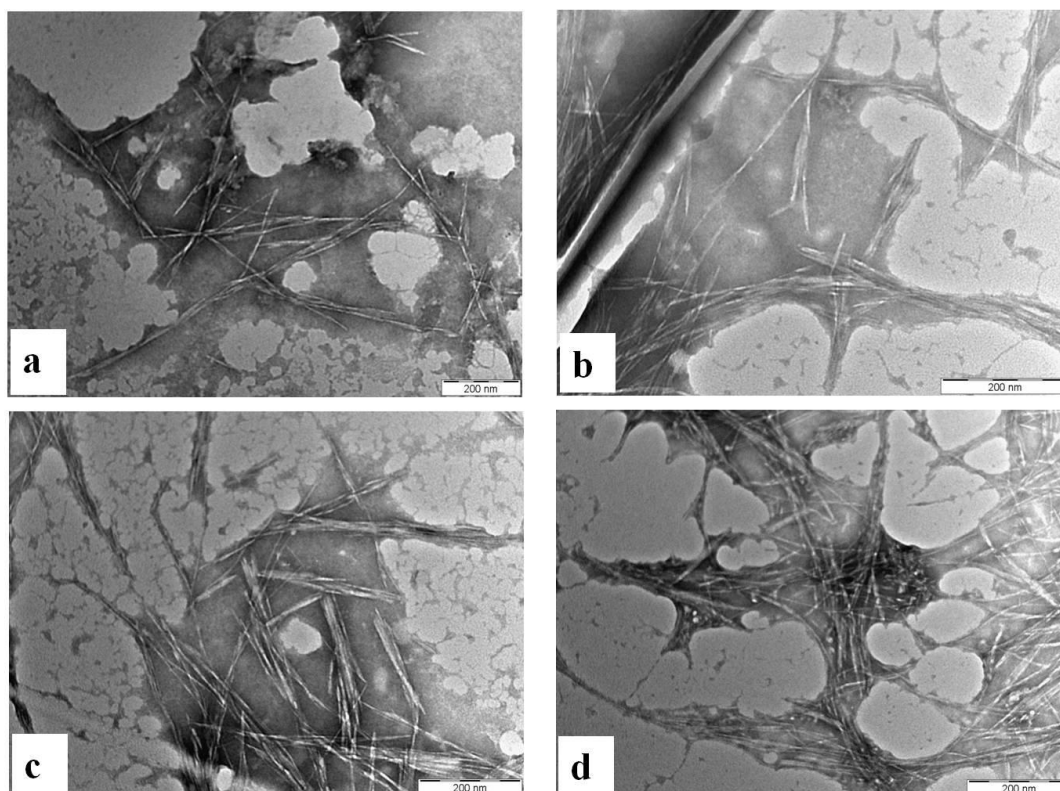


Fig. 2. TEM images of CNW samples (a) CNW-15, (b) CNW-30, (c) CNW-45, and (d) CNW-60

The results in Table 2 show that the aspect ratio (L/D) of OPF-CNWs was comparable with the CNW extracted from other biomass. The aspect ratio of all the CNWs samples was more than 10, which is the minimum required value for nanowhisker for adequate transfer of mechanical stress at matrix/filler interface of nanocomposites (Johari *et al.* 2016). High aspect ratio of CNW is vital because it strengthens various mechanical properties of the composites. CNW improves the functional properties of reinforced materials by introducing crystallinity in nanocomposites (Johar *et al.* 2012). Table 2 also shows that there was remarkable difference in the length of CNW as the hydrolysis duration time changed.

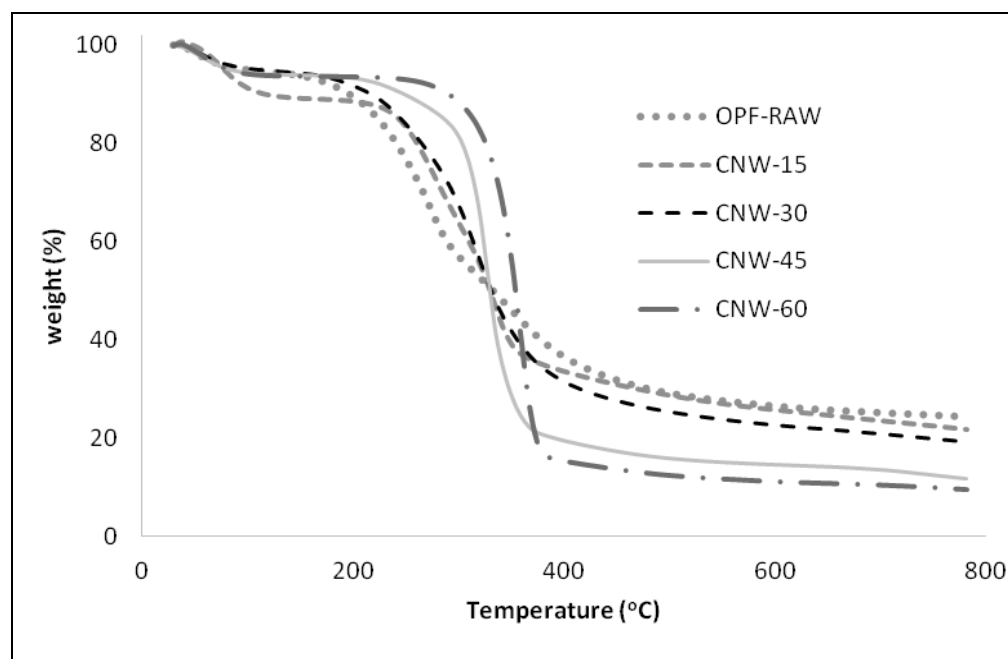
Table 2. Dimensions of CNW Derived from OPF and other Lignocellulose Sourced Fibres

| Source of CNW | Source of CNW | Yield (%) | Length (nm) | Diameter (nm) | L/D | Reference |
|-----------------|---------------|-------------|---------------|---------------|-------|---------------------------|
| Eucalyptus Pulp | NCC-45 | - | 98.47± 3.8 | 3.0 ± 1.03 | 32.82 | (Zeni <i>et al.</i> 2016) |
| Pea hull fiber | | - | 240–400 | 7–12 | 37 | (Chen <i>et al.</i> 2015) |
| Black spruce | | - | 141 ± 6 | 5 | 23 | (Viet <i>et al.</i> 2007) |
| OPF | CNW-15 | 42.47± 0.2 | 106.33 ± 1.25 | 6.01 ± 0.40 | 17.70 | Present study |
| | CNW-30 | 38.71± 0.5 | 111 ± 0.82 | 7.44 ± 0.17 | 14.93 | |
| | CNW-45 | 35.81 ± 0.3 | 178 ± 5.66 | 5.49 ± 0.14 | 32.40 | |
| | CNW-60 | 27.35± 0.2 | 146 ± 3.74 | 5.20 ± 0.07 | 28.06 | |
| EFB | CNW-120 | - | 194 ± 70 | 5.5 ± 1.5 | 39 | (Rosa <i>et al.</i> 2010) |
| | CNW-150 | - | 179 ± 59 | 5.5 ± 1.4 | 36 | |
| | CNW-180 | - | 204 ± 76 | 5.6 ± 1.3 | 41 | |

As a result of strong conditions of acid hydrolysis, cellulose fibres are usually characterized with cleavage at the amorphous region of microfibrils transversely, which resulted in reduction in fibre diameter from microns to nanometers (Chen *et al.* 2014; Fahma *et al.* 2011). The transverse cleavage of amorphous part during hydrolysis might explain that why the fibre length increases and fibre diameter reduces with hydrolysis time (Fahma *et al.* 2011; French *et al.* 2013). Sulphuric acid penetrated the amorphous region, causing hydrolytic cleavage of the glycosidic bonds thereby releasing the individual crystalline fibres. (Li *et al.* 2015).

Thermal Analysis

Thermal stability of the raw OPF sample and CNW produced at different hydrolysis time is shown in Fig 3.

**Fig. 3.** TGA curves of raw and CNW samples at different hydrolysis time.

The TGA curves showed that there were three stages of weight loss (Fig. 3). First stage was attributed to the moisture removal from fibres between 50 °C to 110 °C. The curves showed additional weight loss in cellulose fibre and nanowhiskers when further heated (Lamaming *et al.* 2015; Zeni *et al.* 2016). The second phase of weight loss is attributed to the hemicellulose and cellulose degradation (Fahma *et al.* 2011; Owolabi *et al.* 2016). The raw OPF, CNW-15, CNW-30, CNW-45, and CNW-60 started to degrade at 202 °C, 222 °C, 212 °C, 215 °C, and 222 °C, respectively. Degradation of raw fibres commenced before the degradation of CNWs. This difference was due to the degradation of wax, pectins, and other extractives present in raw biomass (Jahan *et al.* 2016). A sharp curve recorded at 290 °C for raw fibre was due to hemicellulose degradation (Banerjee *et al.* 2011). The high thermal stability of CNWs could be due to the higher degree of crystallinity after the hydrolysis (Jonoobi *et al.* 2010). The thermal analysis of raw fiber showed that higher percentage of weight residue was left at the end of thermal degradation as compared to the CNWs. This was due to the presence of lignin in raw samples.

Crystallinity of the Cellulose Nanowhiskers

Results of XRD analysis of CNWs are shown in Fig. 4. The graph shows two peaks that are characteristic of cellulose I type of natural fibre, as independently reported by Fahma *et al.* (2011) and French *et al.* (2013), indicating that hydrolysis did not alter the natural cellulose structure in CNWs.

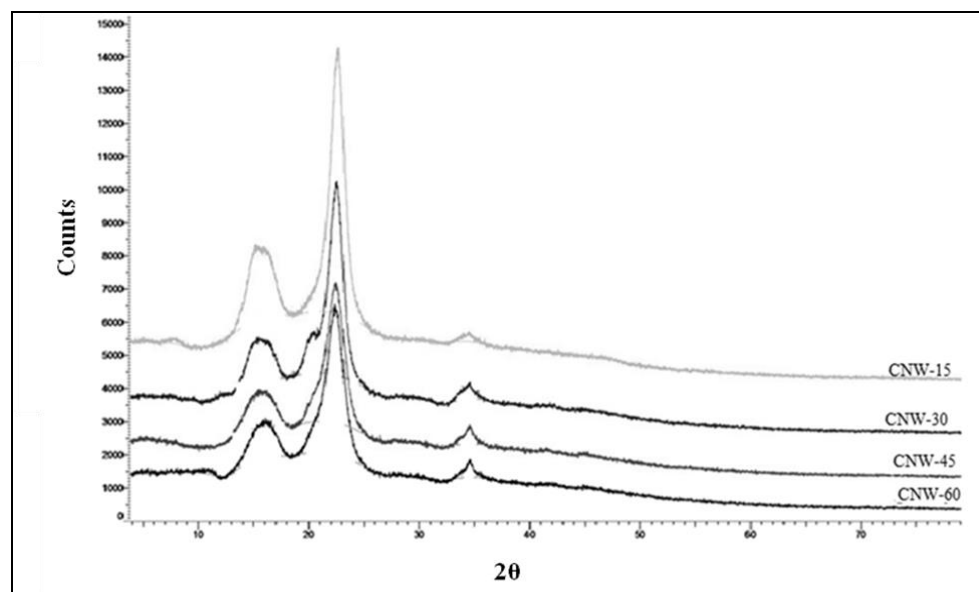


Fig. 4. XRD curve of cellulose nanowhiskers at different hydrolysis time

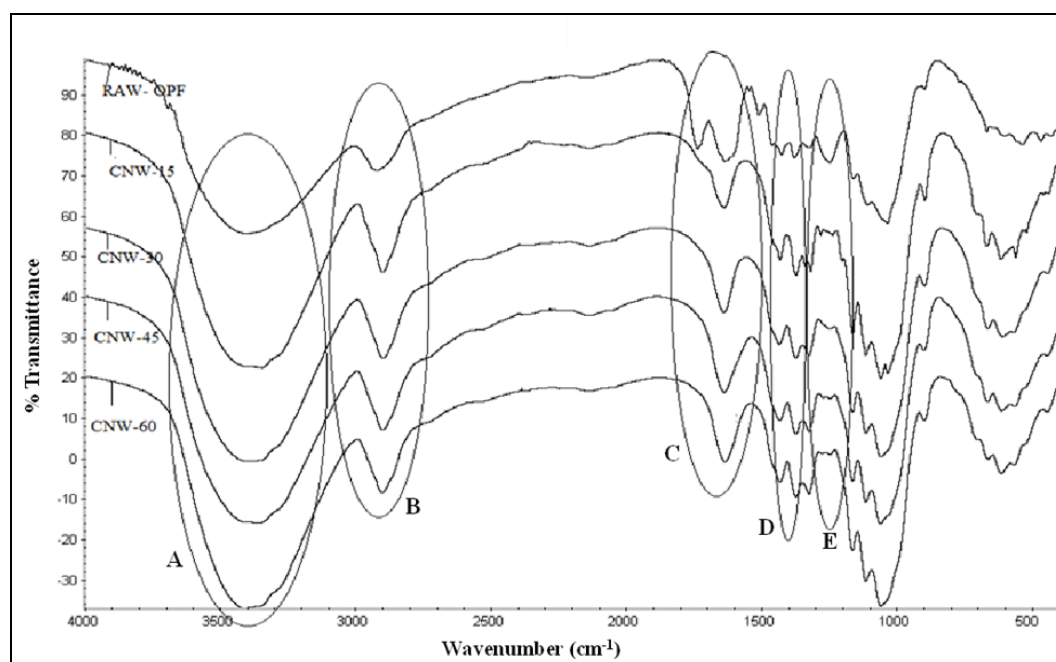
Furthermore, decrease in crystallinity size of nanowhiskers was observed with increase in hydrolysis time (Table 3). Similar results were earlier reported for the extraction of CNW using different hydrolysis time for other oil biomass (Table 3). The progressive increase in the percent crystallinity was attributed to the cleavage of glycosidic bonds as the sulphuric acid penetrates the amorphous region of the cellulose (Fahma *et al.* 2011; French 2014). It was also observed that there was no significant difference between crystallinity % of CNW-45 and CNW-60.

Table 3. Crystallinity Size and Crystallinity % of the CNW

| | CNW | Crystallinity % | Crystallinity size (nm) |
|------------------|--------|---------------------------|--------------------------|
| OPF | CNW-15 | 50.63 ± 0.25 ^c | 7.55 ± 0.42 ^a |
| | CNW-30 | 66.9 ± 0.72 ^b | 6.87 ± 0.40 ^b |
| | CNW-45 | 69.5 ± 0.51 ^a | 6.40 ± 0.21 ^b |
| | CNW-60 | 69.93 ± 0.15 ^a | 4.57 ± 0.17 ^c |
| EFB ¹ | CNW-15 | 58.78 ± 0.70 | 2.51 ± 1.03 |
| | CNW-30 | 56.97 ± 0.34 | 2.05 ± 0.95 |
| | CNW-60 | 54.22 ± 1.46 | 2.05 ± 0.89 |
| | CNW-90 | 53.83 ± 2.03 | 1.96 ± 0.85 |
| OPT ² | CNW-45 | 69.61 - 68.07 | |

Values are means of standard deviation (± SD); Values within the same column with different superscript letters were significantly different ($p < 0.05$).; (¹Fahma *et al.* 2011; ²Lammaming *et al.* 2015)

The crystallinity index of CNW extracted from oil palm trunk (OPT) by Lammaming *et al.* (2015) was higher than the crystallinity observed in the present study, which could be attributed to the mild pre-treatment of OPT by hot water. The crystallinity size was reduced with hydrolysis (Table 3). It was reported that mechanical pre-treatment such as pulping of fibres changes the crystallinity size (Owolabi *et al.* 2016). Change in size was attributable to the breaking of intermolecular hydrogen bonds of cellulose during refining, causing the collapse of the crystal structure of the cellulose fibre (Li *et al.* 2015; French 2014). This phenomenon increases with the acid hydrolysis time, and hence a reduction in crystalline sizes was observed. The crystalline region is highly resistant to acid hydrolysis; however, it might get slightly degraded by acid hydrolysis at high acid concentrations and longer exposure time (Elazzouzi-Hafraoui *et al.* 2007; Chen *et al.* 2014). In the present study, degradation of crystalline region occurred as indicated by a decrease in crystallinity size of the CNWs.

**Fig. 5.** FT-IR spectra for CNWs isolated from OPF by hydrolysis

FTIR

The FTIR spectra of CNWs isolated from OPF are shown in Fig. 5. Similarity in spectral profiles and comparable intensities of CNWs and raw fiber confirmed that the sulphuric acid hydrolysis did not significantly change the chemical nature of the nanowhiskers. This result is in agreement with already published reports on nanocrystal formation through acid hydrolysis of oil palm biomass and lignocellulose biomass (Fahma *et al.* 2011; Yang *et al.* 2014; Li *et al.* 2015; Zeni *et al.* 2016; Lamaming *et al.* 2015).

FTIR spectra of the CNWs bands were dominated by a peak between 3381 and 3406 cm^{-1} due to OH groups stretching vibrations as highlighted from section A on the spectra profile. This peak was observed in all samples due to the presence of hydroxyl groups in cellulose, hemicelluloses, and lignin (Zoppe *et al.* 2014; Lamaming *et al.* 2015). Bands between 2904 and 2921 cm^{-1} (section B) were assigned to saturated aliphatic C-H stretching characteristics of methylene groups in cellulose (Habibi *et al.* 2010). The peak at 1734 cm^{-1} (section C) in the raw OPF and as shoulder spectra in CNW-15 spectra is assigned to the C=O stretching of the acetyl of uronic ester groups in hemicelluloses or to the ester linkage of carboxylic group of the ferulic and -coumaric acids of lignin that is non-conjugated to the aromatic ring (Wang and Chen 2013). This spectra peak was further reduced to a shoulder in CNW-30, and it later disappears in CNW-45 and CNW-60, indicating the removal of hemicellulose. The presence of carboxylate groups was indicated by the peak from 1608 to 1640 cm^{-1} in CNW (section D) and assigned to the bending mode of absorbed water (Khalil *et al.* 2014b). The peak at 1598 cm^{-1} and 1426 cm^{-1} (section E) corresponded with C-H deformations and aromatic ring vibrations in the nanowhiskers, respectively (Qiao *et al.* 2016, Pouyet *et al.* 2014). Such absorbance is common for all the nanowhisiker lignin fractions and indicates the identical degree of aromaticity. This is evidenced by the amount of the residual char after the thermal degradation of the nanowhiskers as demonstrated by TGA (French and Cintrón 2013). The increased spectra bands at 897 cm^{-1} in all CNWs spectra could be attributed to the β -glycosidic linkages of glucose ring of cellulose indicating that the nanowhiskers have high cellulose content (Zeni *et al.* 2016; Habibi 2014).

CONCLUSIONS

1. Cellulose nanowhiskers were successfully isolated from waste oil palm fronds, which are abundant biomass in Malaysia, through sulphuric acid hydrolysis using four different time lengths.
2. Results showed that the crystallinity size and aspect ratio changed with hydrolysis time, indicating that hydrolysis is an important factor in determining the properties of cellulose nanowhiskers (CNW).
3. Hydrolysis did not affect the cellulose 1 polymorph of nanowhiskers.
4. Among all the CNWs, CNW-45 might be the best possible choice as a reinforcing agent due to its highest aspect ratio, crystallinity percentage, and moderate crystallinity size.
5. The cheap and general availability of the biomass will contribute towards economic advantage of cellulose nanowhiskers from oil-palm frond (OPF).

ACKNOWLEDGMENTS

The authors would like to thank the Universiti Sains Malaysia (USM) for the awarded Postdoctoral Fellowship. Authors also like to extend their thanks to the research collaboration between School of Industrial Technology, USM, Malaysia and School of Life Sciences and Technology, Institut Teknologi Bandung, Indonesia. The authors are gratefully acknowledged Universiti Sains Malaysia, Penang, Malaysia for providing Research University Grant (RUI-1001/PTEKIND/814255).

REFERENCES CITED

- Abdul Khalil, H., Siti Alwani, M., Ridzuan, R., Kamarudin, H., and Khairul, A. (2008). "Chemical composition, morphological characteristics, and cell wall structure of Malaysian oil palm fibers," *Polymer-Plastics Technology and Engineering* 47, 273-280. DOI: 10.1080/03602550701866840
- Aprilia, N. S., Hossain, M. S., Abdullah, C. K., Khalil, H. A., Rosamah, E., Dungani, R., Davoudpour, Y., and Zaidul, I. M. (2015). "Environmental durability of vinyl ester composites filled with carbonized jatropha seed shell," *BioResources* 10(2), 2350-2359. DOI: 10.15376/biores.10.2.2350-2359
- Banerjee, G., Car, S., Scott-Craig, J. S., Hodge, D. B., and Walton, J. D. (2011). "Alkaline peroxide pretreatment of corn stover: Effects of biomass, peroxide, and enzyme loading and composition on yields of glucose and xylose," *Biotechnology for Biofuels* 4, 1. DOI: 10.1186/1754-6834-4-16
- Battista, O., and Smith, P. (1962). "Microcrystalline cellulose," *Ind. Eng. Chem.* 54(9), 20-29. DOI: 10.1021/ie50633a003
- Battista, O. A. (1950). "Hydrolysis and crystallization of cellulose," *Ind. Eng. Chem.* 42(3), 502-507. DOI: 10.1021/ie50483a029
- Brioude, M. M., Roucoules, V., Haidara, H., Vonna, L., and Laborie, M.-P. (2015). "Role of cellulose nanocrystals on the microstructure of maleic anhydride plasma polymer thin films," *ACS Appl. Mater. Interfaces* 7(25), 14079-14088. DOI: 10.1021/acsami.5b03302
- Chen, L., Wang, Q., Hirth, K., Baez, C., Agarwal, U. P., and Zhu, J. (2015). "Tailoring the yield and characteristics of wood cellulose nanocrystals (CNC) using concentrated acid hydrolysis," *Cellulose* 22(3), 1753-1762. DOI: 10.1007/s10570-015-0615-1
- Chen, S., Schueneman, G., Pipes, R. B., Youngblood, J., and Moon, R. J. (2014). "Effects of crystal orientation on cellulose nanocrystals – Cellulose acetate nanocomposite fibers prepared by dry spinning," *Biomacromolecules* 15(10), 3827-3835. DOI: 10.1021/bm501161v
- Davoudpour, Y., Hossain, S., Khalil, H. A., Haafiz, M. M., Ishak, Z. M., Hassan, A., and Sarker, Z. I. (2015). "Optimization of high pressure homogenization parameters for the isolation of cellulosic nanofibers using response surface methodology," *Ind. Crop. Prod.* 74, 381-387. DOI: 10.1016/j.indcrop.2015.05.029
- Eichhorn, S., Dufresne, A., Aranguren, M., Marcovich, N., Capadona, J., Rowan, S., and Renneckar, S. (2010). "Review: Current international research into cellulose nanofibres and nanocomposites," *J. Mater. Sci.* 45(1), 1-33. DOI: 10.1007/s10853-009-3874-0

- Fahma, F., Iwamoto, S., Hori, N., Iwata, T., and Takemura, A. (2011). "Effect of pre-acid-hydrolysis treatment on morphology and properties of cellulose nanowhiskers from coconut husk," *Cellulose* 18(2), 443-450. DOI: 10.1007/s10570-010-9480-0
- French, A. D. (2014). "Idealized powder diffraction patterns for cellulose polymorphs," *Cellulose* 21(2), 885-896. DOI: 10.1007/s10570-013-0030-4
- French, A. D., and Cintrón, M. S. (2013). "Cellulose polymorphy, crystallite size, and the Segal crystallinity index," *Cellulose* 20(1), 583-588. DOI: 10.1007/s10570-012-9833-y
- Habibi, Y. (2014). "Key advances in the chemical modification of nanocellulose," *Chem. Soc. Rev.* 43(5), 1519-1542. DOI: 10.1039/C3CS60204D
- Habibi, Y., Lucia, L. A., and Rojas, O. J. (2010). "Cellulose nanocrystals: Chemistry, self-assembly, and applications," *Chem. Rev.* 110(6), 3479-3500. DOI: 10.1021/cr900339w
- Haafiz, M. M., Hassan, A., Zakaria, Z., and Inuwa, I. (2014). "Isolation and characterization of cellulose nanowhiskers from oil palm biomass microcrystalline cellulose," *Carbohydrate Polymers* 103, 119-125. DOI: 10.1016/j.carbpol.2013.11.055
- Hashim, R., Saari, N., Sulaiman, O., Sugimoto, T., Hiziroglu, S., Sato, M., and Tanaka, R. (2010). "Effect of particle geometry on the properties of binderless particleboard manufactured from oil palm trunk," *Materials & Design* 31, 4251-4257. DOI: 10.1016/j.matdes.2010.04.012
- Jahan, M. S., Mostafizur Rahman, J. N. M., Islam, M., and Quaiyyum, M. A. (2016). "Chemical characteristics of ribbon retted jute and its effect on pulping and papermaking properties," *Ind. Crop. Prod.* 84, 116-120. DOI: 10.1016/j.indcrop.2016.01.054
- Johar, N., Ahmad, I., and Dufresne, A. (2012). "Extraction, preparation and characterization of cellulose fibres and nanocrystals from rice husk," *Ind. Crop. Prod.* 37(1), 93-99. DOI: 10.1016/j.indcrop.2011.12.016
- Johari, A. P., Kurmvanshi, S., Mohanty, S., and Nayak, S. (2016). "Influence of surface modified cellulose microfibrils on the improved mechanical properties of poly (lactic acid)," *Int. J. Biol. Macromol.* 84, 329-339. DOI: 10.1016/j.ijbiomac.2015.12.038
- Jonoobi, M., Harun, J., Mathew, A. P., and Oksman, K. (2010). "Mechanical properties of cellulose nanofiber (CNF) reinforced polylactic acid (PLA) prepared by twin screw extrusion," *Composites Science and Technology* 70, 1742-1747. DOI: 10.1016/j.compscitech.2010.07.005
- Khalil, H. A., Hossain, M. S., Rosamah, E., Norulaini, N. N., Leh, C. P., Asniza, M., Davoudpour, Y., and Zaidul, I. (2014a). "High-pressure enzymatic hydrolysis to reveal physicochemical and thermal properties of bamboo fiber using a supercritical water fermenter," *BioResources* 9(4), 7710-7720. DOI: 10.15376/biores.9.4.7710-7720
- Khalil, H. A., Dungani, R., Mohammed, I. A., Hossain, M. S., Aprilia, N. S., Budiarmo, E., and Rosamah, E. (2014b). "Determination of the combined effect of chemical modification and compression of agatis wood on the dimensional stability, termite resistance, and morphological structure," *BioResources* 9(4), 6614-6626. DOI: 10.15376/biores.9.4.6614-6626
- Khan, S. A., Hussain, M. Z., Prasad, S., and Banerjee, U. (2009). "Prospects of biodiesel production from microalgae in India," *Renew. Sust. Energ. Rev.* 13(9), 2361-2372. DOI: 10.1016/j.rser.2009.04.005

- Lamaming, J., Hashim, R., Sulaiman, O., Leh, C. P., Sugimoto, T., and Nordin, N. A. (2015). "Cellulose nanocrystals isolated from oil palm trunk," *Carbohydr. Polym.* 127, 202-208. DOI: 10.1016/j.carbpol.2015.03.043
- Law, K.-N., Daud, W. R. W., and Ghazali, A. (2007). "Morphological and chemical nature of fiber strands of oil palm empty-fruit-bunch (OPEFB)," *BioResources* 2, 351-362.
- Li, B., Xu, W., Kronlund, D., Määttänen, A., Liu, J., Smått, J.H., Peltonen, J., Willför, S., Mu, X., and Xu, C. (2015). "Cellulose nanocrystals prepared via formic acid hydrolysis followed by TEMPO-mediated oxidation," *Carbohydr. Polym.* 133, 605-612. DOI: 10.1016/j.carbpol.2015.07.033
- Liu, M., Yang, J., Liu, Z., He, W., Liu, Q., Li, Y., and Yang, Y. (2015). "Cleavage of covalent bonds in the pyrolysis of lignin, cellulose, and hemicellulose," *Energy & Fuels* 29, 5773-5780. DOI: 10.1021/acs.energyfuels.5b00983
- Mustafa, M. T., Wahab, R., Sudin, M., Khalid, I., and Kamal, N. A. M. (2011). "Anatomical properties and microstructures features of four cultivated bamboo *Gigantochloa* species," *J. Asian Sci. Res.* 1(7), 328-339.
- Naran, R., Black, S., Decker, S. R., and Azadi, P. (2009). "Extraction and characterization of native heteroxylans from delignified corn stover and aspen," *Cellulose* 16, 661-675. DOI: 10.1007/s10570-009-9324-y
- Osorio-Madrado, A., Eder, M., Rueggeberg, M., Pandey, J. K., Harrington, M. J., Nishiyama, Y., and Burgert, I. (2012). "Reorientation of cellulose nanowhiskers in agarose hydrogels under tensile loading," *Biomacromolecules* 13(3), 850-856. DOI: 10.1021/bm201764y
- Owolabi, A. W. T., Arniza, G., wan Daud, W., and Alkharkhi, A. F. (2016). "Effect of alkaline peroxide pre-treatment on microfibrillated cellulose from oil palm fronds rachis amenable for pulp and paper and bio-composite production," *BioResources* 11(2), 3013-3026.
- Peleteiro, S., Rivas, S., Alonso, J. L., Santos, V., and Parajó, J. C. (2015). "Utilization of ionic liquids in lignocellulose biorefineries as agents for separation, derivatization, fractionation, or pretreatment," *J. Agr. Food. Chem.* 63(37), 8093-8102. DOI: 10.1021/acs.jafc.5b03461
- Pouyet, F., Chirat, C., Potthast, A., and Lachenal, D. (2014). "Formation of carbonyl groups on cellulose during ozone treatment of pulp: Consequences for pulp bleaching," *Carbohydr. Polym.* 109, 85-91. DOI: 10.1016/j.carbpol.2014.02.082
- Qiao, C., Chen, G., Zhang, J., and Yao, J. (2016). "Structure and rheological properties of cellulose nanocrystals suspension," *Food Hydrocolloid.* 55, 19-25. DOI: 10.1016/j.foodhyd.2015.11.005
- Rosa, M. F., Medeiros, E. S., Malmonge, J. A., Gregorski, K. S., Wood, D. F., Mattoso, L. H. C., Glenn, G., Orts, W. J., and Imam, S. H. (2010). "Cellulose nanowhiskers from coconut husk fibers: Effect of preparation conditions on their thermal and morphological behavior," *Carbohydr. Polym.* 81(1), 83-92. DOI: 10.1016/j.carbpol.2010.01.059
- Sèbe, G., Ham-Pichavant, F. d. r., Ibarboure, E., Koffi, A. L. C., and Tingaut, P. (2012). "Supramolecular structure characterization of cellulose II nanowhiskers produced by acid hydrolysis of cellulose I substrates," *Biomacromolecules* 13(2), 570-578. DOI: 10.1021/bm201777j

- Stuart, A. R., and Erb, R. M. (2014). "Bioinspired materials that self-shape through programmed microstructures," *Soft Matter* 10(9), 1284-1294. DOI: 10.1039/C3SM51883C
- Viet, D., Beck-Candanedo, S., and Gray, D. G. (2007). "Dispersion of cellulose nanocrystals in polar organic solvents," *Cellulose* 14(2), 109-113. DOI: 10.1007/s10570-006-9093-9
- Wang, N., and Chen, H.-Z. (2013). "Manufacture of dissolving pulps from cornstalk by novel method coupling steam explosion and mechanical carding fractionation," *Bioresour. Technol.* 139, 59-65. DOI: 10.1016/j.biortech.2013.04.015
- White, J. E., Catallo, W. J., and Legendre, B. L. (2011). "Biomass pyrolysis kinetics: A comparative critical review with relevant agricultural residue case studies," *J. Anal. Appl. Pyrol.* 91(1), 1-33. DOI: 10.1016/j.jaap.2011.01.004
- Xu, X., Wang, H., Jiang, L., Wang, X., Payne, S. A., Zhu, J., and Li, R. (2014). "Comparison between cellulose nanocrystal and cellulose nanofibril reinforced poly (ethylene oxide) nanofibers and their novel shish-kebab-like crystalline structures," *Macromolecules* 47(10), 3409-3416. DOI: 10.1021/ma402627j
- Yang, S., Tang, Y., Wang, J., Kong, F., and Zhang, J. (2014). "Surface treatment of cellulosic paper with starch-based composites reinforced with nanocrystalline cellulose," *Ind. Eng. Chem. Res.* 53(36), 13980-13988. DOI: 10.1021/ie502125s
- Zeni, M., Favero, D., Pacheco, K., and Grisa, A. (2016). "Preparation of microcellulose (Mcc) and nanocellulose (Ncc) from *Eucalyptus* kraft Ssp pulp," *Polym. Sci.* 1(1:7).
- Zoppe, J. O., Ruottinen, V., Ruotsalainen, J., Rönkkö, S., Johansson, L.-S., Hinkkanen, A., Järvinen, K., and Seppälä, J. (2014). "Synthesis of cellulose nanocrystals carrying tyrosine sulfate mimetic ligands and inhibition of alphavirus infection," *Biomacromolecules* 15(4), 1534-1542. DOI: 10.1021/bm500229d

Article submitted: April 14, 2016; Peer review completed: May 29, 2016; Revised version received and accepted: June 10, 2016; Published: June 29, 2016.
DOI: 10.15376/biores.11.3.6742-6755